SPATIAL POINT PROCESSES AND GRAPH BASED STATISTICAL FEATURES

Tuomas Rajala

Preprint 385 January 2010

2000 *Mathematics Subject Classification.* 60G55, 62-07, 62M30.

ISSN 1457-9235

SPATIAL POINT PROCESSES AND GRAPH BASED STATISTICAL FEATURES

Tuomas Rajala

January 2010

2000 *Mathematics Subject Classification.* 60G55, 62-07, 62M30.

Spatial point processes and graph based statistical features

Tuomas Rajala
Department of Mathematics and Statistics, University of Jyväskylä, Finland
tuomas.rajala@jyu.fi

January 14, 2010

Abstract

Spatial point processes are stochastic models for point patterns, systems of points scattered in $\mathbb{R}^d$. A point process can be used as a generating stochastic mechanism for additional spatial random systems such as random tessellations, random fields and random graphs, which are collectively called secondary structures of point processes. Secondary structures have a role in the statistical analysis of point processes, e.g. in the form of statistical summaries based on tessellations, and in a method called regionalisation which bridges point pattern statistics with geostatistics. In this study the objective is to use geometric graphs together with graph-based summaries in the statistical analysis of small-scale properties of point patterns. The functional summaries of this study are connectivity function, cumulative connectivity function and clustering function. The concepts and their estimators are given, their properties are discussed, and a simulation study is conducted. The simulation experiment gives evidence that the graph-theoretical summaries are able to detect differences between point patterns where the second-order statistics such as Ripley's K or pair-correlation function fail. An `R` library has been developed for the computation of the graph-based summaries.

Keywords: Spatial point processes, graphs, complete spatial randomness.

2010 Mathematics Subject Classification 60G55, 62-07, 62M30

1 Introduction

Spatial point patterns are statistical data in the form of collections of points, representing locations or objects in $\mathbb{R}^d$ with $d \geq 2$, whilst spatial point processes are models for such data. Modern statistical analysis of point patterns utilises the theory, models and efficient use of simulation of point processes, see e.g. Møller and Waagepetersen (2003); Illian et al. (2008). This study focuses on the use of graph theory as model characteristics and data summaries in point process statistics.

In the applications of point process statistics many other techniques are surpassed by the second-order methods. These consists of Ripley's K-function (Ripley, 1976) and pair-correlation function (e.g. Stoyan et al., 1995) which are efficient tools for detecting clustered or regular spacings at a variety of scales. The second-order analysis is based on pairs of points, and as such restrict their applicability when specific hypotheses such as alingments of points are under consideration. A well known counter-example by Baddeley and Silverman (1984) is the Cell model which has the same second-order structure as the Poisson process, but produces distinctly non-Poisson patterns. To tackle these limitations more elaborate summaries have been introduced, such as the third-order summary by Schladitz and Baddeley (2000).

Secondary structures of point processes are models where the randomness of the point process is used to create a new type of random structure through a known mapping. The most common objective is to employ new stochastic models for various random structures, but dual to that, the underlying point processes can be studied through the transformed process. An example is to transform a point process N to a random set X via Minkovski addition of R-discs. Then the the analysis of the random set X by means of morphological summaries with various values of R gives information on the underlying point process N. These morphological characteristics, containing the spherical contact distribution function, has been studied by Mecke and Stoyan (2005). Further examples of the use of secondary structures of point processes are statistics based on tessellations (Okabe et al. (2000)) and regionalization through

intensity estimation or mark-sum measure (Stoyan et al. (1995)) which brings the point processes to geostatistics.

In this study secondary structure of point processes are given by geometric graphs as outlined in Illian et al. (2008). Geometric graphs are generated from a pattern by means of a neighbourhood relation and then features of the graph are used to study the underlying point process. Three model characteristics are considered. Connectivity function, which first appeared in Illian et al. (2008), is studied in detail and a choice of a parameter used in the construction of the graph is suggested. Second, a new cumulative connectivity function is put forward. Third, the clustering function, based on a graph theoretical characteristic, is developed and applied to spatial analysis emphasizing the interplay between statistics of point patterns and graphs.

For the three characteristics considered, estimators are given and a deviation test based simulation study is conducted to analyse their behaviour. The study points out that the use of graph-based summaries is not without problems but, if correctly constructed, they can surpass the second-order point process statistics for some important data. Hence graph theoretical summaries should be included into the toolbox of point process statistics. This in mind, an implementation of the summaries is released online as a free `R` package.

The paper is organized as follows. In Section 2 preliminaries of point processes and graphs are recalled. The graph-based characteristics and their empirical counterparts are presented in Section 3. In Section 4 the new summaries are studied with a simulation experiment. Section 5 is for discussion.

2 Preliminaries

We write B and B_i for a Borel sets of $\mathbb{R}^d$, $d = 2, 3$, and ν for the Lebesgue measure. The notation $b(x, r)$ is used for an open ball centred at x and having radius $r > 0$, and $||\cdot||$ for the d-dimensional Euclidian distance.

2.1 Point processes

Let $N = \{x_1, ..., x_n\} \subset \mathbb{R}^d$, $n \in \mathbb{N}$, be a simple, stationary and isotropic *point process* with intensity $\lambda > 0$. Simple means that duplicate locations are not allowed, stationarity and isotropy imply that $N + s = \{x_i + s\}$ and $\mathbf{r}N = \{\mathbf{r}x_i\}$ have the same distribution as N with respect to any $s \in \mathbb{R}^d$ and rotation $\mathbf{r}$, respectively. Let $\mathbf{x}$ stand for a realisation of N, termed point *pattern*. Write the cardinality $N(B) := |N \cap B|$ for any B. The observation window is assumed to be $W := [0, 1]^d$ if not otherwise stated. If the points x_i have marks attached we let $M := \{[x_i; m_i]\}$ denote the corresponding *marked point process*. We assume that the marks are scalar, $m_i \in \mathbb{R}$. If especially $m_i \in \{1, 2, \ldots, k\}$ we call the process *multivariate*.

The point process model for complete spatial randomness (CSR) is the *Poisson process*, characterised by parameter $\lambda > 0$ and the following two features: 1) For any B the integer valued random variable $N(B)$ is a Poisson distributed random variable with intensity $\lambda\nu(B)$, 2) For each disjoint pair B_1 and B_2 the random variables $N(B_1)$ and $N(B_2)$ are independent. The second property describes the independent random scattering of the points.

The theory of spatial point processes and various aspects of its application can be found e.g. in Stoyan et al. (1995), Møller and Waagepetersen (2003), Daley and Vere-Jones (2005) and Illian et al. (2008).

2.2 Point process generated geometric graphs

We use *graphs* to structure point patterns (see e.g. Marchette, 2004). Define a graph to be a dual $G := (V, E)$ where V is a non-empty, countable set called the *node* set and E is a set of ordered pairs $\{(x_i, x_j) : x_i, x_j \in V\}$ called the *edge* set. E can be given by some rule, usually by a relation $\cdot \leftrightarrow \cdot$ on V. We assume $\leftrightarrow$ is symmetric and irreflexive. In particular, for $V \subset \mathbb{R}^d$ and $R > 0$, define a relation

$$x_i \overset{R}{\leftrightarrow} x_j \iff ||x_i - x_j|| \leq R.$$

Call the corresponding graph the *geometric graph*.

Denote the *neighbourhood* of $x_i \in V$ by $ne(x_i) := \{x_j \in V : x_i \leftrightarrow x_j\}$. Define a *path* from x to y as a set of distinct, subsequently connected nodes $\{x_1, x_2, \ldots, x_k : x \leftrightarrow x_1, \ldots, x_k \leftrightarrow y\}$. If there exists a path between x and y we write $x \sim y$. The path relation $\sim$ divides the graph G into pairwise disconnected *components* $C_l := \{S \subseteq V : \forall x_i, x_j \in S \; x_i \sim x_j\}$. Write also $C(x_i) := \{x_j : x_i \sim x_j\}$, and denote the components of G by $\Gamma(G) := \bigcup_{x_i \in V} C(x_i)$. The graph is *completely connected* if $|\Gamma(G)| = 1$, meaning that all node pairs are path connected.

Following Illian et al. (2008) we use graphs as a secondary structure for point processes. Let $V = N$ be a stationary (marked) point process, and set $G(N) := (N, E)$ to be the new randomly behaving geometric graph. Note the distinction to the classical *Erdős-Rényi random graph* (Erdős and Rényi, 1959) in which the edges are independently present with fixed probability p, instead of the complex dependencies when the connection probability depends on the spatial distribution of the points.

Of great interest in spatial point pattern analysis are the distribution characteristics of other points with respect to a typical (or randomly chosen) point. An example is the distribution of the typical distance to the nearest neighbour from any $x \in N$, understood as statistically indistinguishable from the value of any other $x' \in N$. Therefore the node level features of a graph $G(N)$ are of interest and one such feature is the *degree* of a node $x_i \in N$

$$\delta(x_i) = \sum_{x_j \in N} \mathbf{1}(x_i \leftrightarrow x_j).$$

Considering the geometric graph with parameter $R > 0$, by the stochasticity and stationarity of the nodes we can write

$$\mathbf{E}_o \delta(o) = \mathbf{E}_o \sum_{x \in N} \mathbf{1}(x \in b(o, R) \setminus \{o\}) = \lambda K(R)$$

which we call the *mean degree characteristic*. Here $\mathbf{E}_o$ is the Palm-expectation (conditioning $o \in N$), and $K(R)$ is the celebrated special case of a second order reduced moment measure known as the *Ripley's K-function* (Ripley, 1976, 1977): The graph does indeed describe the point process.

In CSR context mathematical properties of the geometric graphs has been studied at least by Penrose (2003), and he implies that the dependency of edges leads to analytical difficulties, for example to problems similar to those of percolation theory. But as the graph is a reasonable extension of a point pattern data and statistical estimation is possible, we proceed to introduce summaries based on this setting.

3 Summaries based on the features of graphs

The secondary structure approach proceeds with two options: 1) Mark a point pattern using information from the graph and study the marked point pattern, or 2) study global topology of the graph. We look at both approaches in turn.

3.1 Cumulative connectivity function

We define a new point pattern summary by extending the idea of mean degree characteristic to a version where the edge connectivity is accompanied by the path connectivity as follows:

Definition 1 *Let N be a stationary and isotropic point process with intensity $\lambda > 0$, and let $G(N)$ be a graph. Set*

$$CC(r) := \lambda^{-1} \mathbf{E}_o \sum_{x \in N \setminus \{o\}} \mathbf{1}(x \in b(o, r) \wedge o \sim x). \tag{1}$$

Call the function $CC(r)$ cumulative connectivity function.

Since the events $\{o \sim x\}$ and $\{o \nsim x\}$ are mutually exclusive, the cumulative connectivity function is related to the K-function: If $\overline{CC}(r)$ denotes the opposite version of $CC(r)$ with $\sim$ replaced by $\nsim$ in (1), then

$$K(r) = CC(r) + \overline{CC}(r). \tag{2}$$

If the graph is completely connected (e.g. geometric graph with $R = \infty$), then $K(r) = CC(r)$. So with a suitable graph the connected components represent clusters and the $CC(r)$ describes their typical structure.

Figure 2 shows the cumulative connectivity function curves for various models, obtained from a simulation experiment of Section 4. The curve for clustered processes ascend quickly above the Poisson process curve because the points typically belong to a large cluster. Regularity of the repulsive processes results in a grid-like connectivity and the curve ascends steadily after the repulsion effect range is passed.

As a cumulative function, small changes of r might not reveal enough details and a function similar to the derivative of K-function, the *pair correlation function*, is considered.

3.2 Connectivity function

The *connectivity function* was first discussed in the book Illian et al. (2008), p. 248. The definition is as follows:

Definition 2 *Let N be a stationary point process. For a given graph $G(N)$, the* connectivity function *$C(r)$ is*

$$C(r) := \mathbf{P}_{x,y}(x \sim y \mid ||x - y|| = r), \qquad r \geq 0. \tag{3}$$

where $\mathbf{P}_{x,y}$ is the 2-point Palm-measure of the process.

As with the $CC(r)$, we generate components in the point pattern using the graph $G(N)$ and look at the second order features inside the components. The behaviour of the function is depicted in Figure 2(center). The connectivity function is a probability and here $C(r) \in [0, 1]$. The geometric graph has a minimum connection radius parameter R, so $C(r) \equiv 1$ for $r \leq R$, and if the graph is completely connected then $C(r) \equiv 1$ for all r.

For the Poisson process function values start declining immediately when range exceeds R. For clustered processes with cluster size larger than R an elevated shoulder occurs. Regular processes' values decrease initially quicker than Poisson values, but exhibit a small stop in decline when range passes the initial repulsion effect. This is because paths can be long in regular patterns (imagine a grid), and furthermore point pairs are abundant just after the repulsion effect range.

For theory of the connectivity function we use the internal marking of the pattern. For a graph $G(N)$ we have the partitioning $\Gamma(G(N))$ to $k = 1, 2, \ldots$ components. Label these components from 1 to k with function $m : \Gamma(G(N)) \to \{1, \ldots, k\}$ according to the distance to origin: $m(C_r) < m(C_s)$ if $\min_{x_i \in C_r} ||x_i|| < \min_{x_i \in C_s} ||x_i||$. By definition a point x_i belongs to only one component so we can mark the points with unique marks $m_i = m(C(x_i))$. Write $\mathbb{M} = m(\Gamma(G(N)))$. We then express the connectivity function as an unscaled *mark correlation function*, see e.g. Stoyan and Stoyan (1994), p. 264: Write $C(r)$ as an expectation over marks

$$C(r) = \sum_m \sum_l [\mathbf{1}(m = l)\mathbf{P}_{o,\mathbf{r}}(m, l)],$$

where $\mathbf{P}_{o,\mathbf{r}}(\cdot, \cdot)$ is the 2-point Palm joint distribution of marks $m, l \in \mathbb{M}$ of two points o and $\mathbf{r}$ distance r apart. From the definition of $\mathbf{P}_{o,\mathbf{r}}$ if follows that

$$C(r) = \sum_m \sum_l \mathbf{1}(m = l)\varrho(r, m, l)/\varrho(r)$$

where $\rho(r)$ is the second order product density of the process at range r, $\rho(r, m, l)$ further considers points distance r apart with the marks m and l. Writing $\varrho_\sim(r) := \sum_m \sum_l \mathbf{1}(m = l)\varrho(r, m, l)$, the previous formula simplifies to

$$C(r) = \frac{\varrho_\sim(r)}{\varrho(r)} \tag{4}$$

whenever the second order product density $\varrho(r) > 0$. The theoretical calculation of $\mathbf{P}_{o,\mathbf{r}}$ is difficult because the path connectivity of two points, also known as percolation, is intractable in most cases as far as we know. In case of the Poisson process, Chandler (1989) derives and Ta et al. (2007) refine a

recursive version: If $C_k(r)$ denotes the probability of connecting two points x, y distance r apart with a path of k edges long, it can be written as

$$C_k(r) = \begin{cases} \mathbf{1}(r < R) & k = 1, \\ (1 - \exp(-\lambda A(r)) \cdot \mathbf{1}(R < r < 2R) & k = 2, \\ (1 - \sum_{i=1}^{k-1} C_i(r))\big(1 - \exp(-\int_{r-R}^{r+R} 2C_{k-1}(x)\lambda x \beta(x, r)dx)\big) & k \geq 3. \end{cases}$$

where $A(r) = |b(o, R) \cap b(\mathbf{r}, R)|$ and $\beta(x, r) = \arccos(\frac{r^2 - x^2 - R^2}{2rx})$. The connectivity function is then $C(r) = \sum_{k=1}^{\infty} C_k(r)$. Penrose (2003) studies the asymptotics of connectivity for the Poisson process and geometric graph, but the results do not implicate a closed form for equation (3).

3.3 Clustering coefficient and clustering function

The *clustering coefficient* is a topological index for graphs introduced by Watts and Strogatz (1998) in the study of communication networks. The definition is as follows:

Let $G = (V, E)$ be a given graph with $|V| = n < \infty$ and recall that $\delta(x)$ is the degree of a node at x. Write for a node $o \in V$

$$\Delta_o := \sum_{x,y \in ne(o)} \mathbf{1}(x \leftrightarrow y) \quad \text{and} \quad \Delta_o^{\max} := \binom{\delta(o)}{2} = \frac{1}{2}\big(\delta(o)^2 - \delta(o)\big)$$

and set

$$c_o := \begin{cases} \frac{\Delta_o}{\Delta_o^{\max}}, & \delta(o) \geq 2, \\ 0, & \delta(o) < 2 \end{cases}.$$

The clustering coefficient c is defined as the average over nodes

$$c := \frac{1}{n} \sum_{x \in V} c_x.$$

In words, Δ_o is the observed number and $\Delta_o^{\max}$ the theoretical maximum number of possible connections amongst the neighbours of a node at o. So the unit of interest in this construction is a triad instead of a pair as in previous summaries. This tool can be adopted for point process analysis.

Definition 3 *Let N be a stationary point process and let $\Delta_{o,r}, \Delta_{o,r}^{\max}$ and $c_{o,r}$ be as above for the geometric graph $G(N)$ with parameter r. Define*

$$c(r) := \mathbf{E}_o c_{o,r}.$$

We call $c(r)$ the clustering function.

Watts and Strogatz (1998) created c to study so called small world networks, in which the path between two arbitrary nodes of the network is shorter than in an Erdős-Rényi graph. However, in our study the coefficient has different interpretation as we have several graphs because the connection radius r varies. The coefficient is a rate of interconnection in the graph, so $c(r)$ could be interpreted as the internal connectivity around a typical point at scale r.

Obviously $c(r) \in [0, 1]$. Clustered processes' values increase immediately above Poisson values, due to high density groups of points leading to large interconnection at small r. The regular processes have little connections at small r, but as the repulsion effect gaps are passed the values also start to increase.

When r increases the nearby clusters merge and the number of clusters decreases. Finally, all point pairs connect and the function, as a ratio of functions of edge counts, converges to a single value. The ratio expected version

$$\tilde{c}(r) := \frac{\mathbf{E}_o \Delta_{o,r}}{\mathbf{E}_o \Delta_{o,r}^{\max}} \tag{5}$$

can be calculated for the Poisson process analytically: It is in $d = 2$

$$\tilde{c}(r) = (1 - \frac{3\sqrt{3}}{4\pi})[1 - e^{-\lambda \pi r^2}(1 + \lambda \pi r^2)]. \tag{6}$$

This can be computed as follows: When $\delta(o) \geq 2$, the numerator equals the T-function of Schladitz and Baddeley (2000), so

$$\begin{aligned}\mathbf{E}_o\Delta_{o,r} &= \frac{1}{2}\mathbf{E}_o \sum_{x,y\in b(o,r)} \mathbf{1}(x \overset{R}{\leftrightarrow} y) \\ &= \lambda^2 T(r) \\ &= \lambda^2 \frac{1}{2}\pi(\pi - \frac{3\sqrt{3}}{4})r^4,\end{aligned}$$

and

$$\mathbf{E}_o\Delta_{o,r}^{\max} = \frac{1}{2}(\mathbf{E}_o[\delta(o)^2] - \lambda K(r)).$$

Because $N(b(o,r) \setminus \{o\}) = \delta(o)$ is by definition Poisson distributed with parameter $\lambda\pi r^2$, we can use Slivnyaek's theorem (see Stoyan et al., 1995) to get

$$\begin{aligned}\mathbf{E}_o[\delta(o)^2] &= \mathbf{Var}_o(\delta(o)) + (\mathbf{E}_o\delta(o))^2 \\ &= \mathbf{Var}(\delta(o)) + (\mathbf{E}\ \delta(o))^2 \\ &= \lambda\pi r^2(\lambda\pi r^2 + 1).\end{aligned}$$

For the Poisson process $K(r) = \pi r^2$, so the expression

$$c_p := \frac{(\pi - \frac{3\sqrt{3}}{4})\lambda^2\pi r^4}{\lambda\pi r^2(\lambda\pi r^2 + 1) - \lambda\pi r^2} = 1 - \frac{3\sqrt{3}}{4\pi} \approx 0.5865$$

is obtained. Finally, when the constant c_p is weighted with the probability of $\{\delta(o) \geq 2\}$,

$$\mathbf{P}_o(\delta(o) \geq 2) = (1 - \exp(-\lambda\pi r^2)[1 + \lambda\pi r^2]),$$

the equation (6) is obtained.

3.4 Estimation

We use nonparametric methods to estimate the summaries statistically for a given point pattern N, observed in a window $W \subseteq \mathbb{R}^d$.

3.4.1 Estimators for the functions

Following Illian et al. (2008) p. 249, an estimator for the connectivity function is

$$\hat{C}(r) = \frac{\hat{\varrho}_{\sim}(r)}{\hat{\varrho}(r)}, \tag{7}$$

given by the equation (4). The denominator is a translation corrected 2nd order product density estimator (Stoyan et al., 1995)

$$\hat{\varrho}(r) = \frac{1}{2\pi r}\sum_{x\neq y} \frac{k_h(r - ||x-y||)}{\nu(W_x \cap W_y)}$$

and it is modified to

$$\hat{\varrho}_{\sim}(r) = \frac{1}{2\pi r}\sum_{x\neq y} \frac{k_h(r - ||x-y||)\mathbf{1}(x \sim y)}{\nu(W_x \cap W_y)}. \tag{8}$$

Here $W_x = \{z - x : z \in W\}$, and the box kernel for smoothing is $k_h(t) = 1/2h$ for $|t| < h$, 0 otherwise. The boundary correction used in (8) is an approximation since the graph could connect two points through an unobserved path outside the window. Hence the estimator (7) is not ratio-unbiased. We have neglected this problem in our simulation study as it is not clear how the correction should be done.

For the cumulative connectivity function we suggest an estimator

$$\widehat{CC}(r) = \hat{\lambda}^{-2} \sum_{x \neq y} \frac{\mathbf{1}(x \sim y)\mathbf{1}(||x-y|| < r)}{\nu(W_x \cap W_y)}. \tag{9}$$

with some intensity estimator $\hat{\lambda}$. The formula is derived from the translation corrected estimator of the K-function.

The clustering function can be estimated using the formula (5) for a given r and $N(W) = n$: We estimate

$$\begin{aligned} \mathbf{E}_o \Delta_{o,r} &\approx \frac{1}{n} \sum_{x \in N \cap W} \sum_{y,z \in b(x,r)} \mathbf{1}(y \overset{r}{\leftrightarrow} z), \\ \mathbf{E}_o \Delta_{o,r}^{\max} &\approx \frac{1}{n} \sum_{x \in N \cap W} \frac{1}{2}\delta(x)(\delta(x)-1). \end{aligned}$$

Minus sampling scheme is used to reduce border effects in estimation of clustering function. As the estimation of (5) uses the ratio of two quantities which are both affected by the same type of border bias, based on the experience in estimation of intensities with ratio-based estimator (Illian et al. (2008), p. 193) the bias is reduced. For the numerator in (5), Schladitz and Baddeley (2000) develop two unbiased estimators based on weighting of the edges close to the border. The first is a three-point version of the translation correction and the second is analogous to the isotropic correction of K-function estimation by Ripley (1977). It is a matter of future studies to investigate how these elaborate methods affect the estimation of $\tilde{c}(r)$.

3.4.2 Choosing the graph parameter R

When working with a constant neighbourhood radius the subjective task of fixing its size is crusial. If the graph is completely connected due to large R, the summaries do not detect any details, and if R is too small the graph is too sparse and the potential clusters are not separated correctly. We studied the use of empirical nearest neighbour distribution mean and median as R by comparing manual cluster selection using visual (subjective) cluster identification and geometric graph clustering. The mean neareast neighbour distance seems to underestimate the clustering by connecting only a few point pairs, especially in a visually very clustered realisation. And as the nearest neighbour distribution of clustered pattern has heavier right tail, the median is less than the mean and the results are even worse.

Using the empirical nearest neighbour distribution in finding a suitable R is also an impractical choice because the distribution depends on the process. This is a problem especially for the connectivity function because R is also the distance under which the function is constant. For example, a clustered process will exhibit smaller nearest neighbour distances than a Poisson process resulting in a smaller mean value and a different starting point for the function.

However, we want to measure the clustering in the scale of the phenomenon, so a value completely independent of the data is not desirable. It is justified to estimate some features of the process as a preliminary step and use them to determine a value for R. The simplest feature to estimate R through is the intensity λ, and this choice does not depend on the higher order structures of the point pattern.

In the simulation experiment study of Section 4 we have set the value of R to $1/\sqrt{\lambda}$. This choise is based on the following reasoning: For a Poisson process $K(r) = \pi r^2$, and the mean degree of a node in a spatial graph with parameter R is $\mathbf{E}_o\delta(o) = \lambda K(R)$. Selecting $R = 1/\sqrt{\lambda}$ the equation

$$\mathbf{E}_o\delta(o) = \lambda K(R) \equiv \pi$$

is obtained. The mean degree of a point in a Poisson process becomes constant with respect to R and λ. Visual inspection of simulation results encourages to use this value, especially over nearest neighbour distance statistics. Figure 1 illustrates the effect of changing the parameter around $R = 1/\sqrt{\lambda}$. For smaller R the value drops to 0 quickly, and for larger R the value stays constant for longer. In CSR case already 60% larger value hides details by connecting most of the points into a single component. Clustered patterns are more robust to the choice of R because they have less points between separated clusters and because even a single point is enough to connect several clusters, resulting in a quick increase in path-connected point pairs.

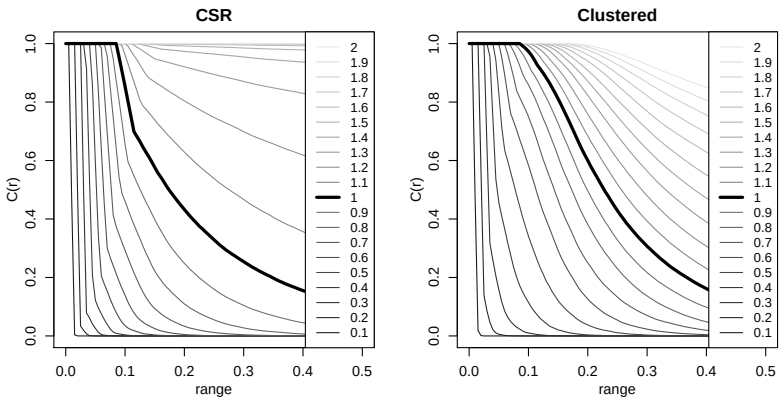

Figure 1: The effect of the graph parameter R. The lines correspond to $C(r)$ when $R = \frac{a}{\sqrt{\lambda}}$ with $a = 0.1, 0.2, \ldots, 1.9, 2.0$, thick line is $a = 1.0$. Curves estimated from 1000 simulations of Poisson process and Thomas cluster process.

4 Simulation study

To assess the usefulness of the graph theoretical summaries we studied how they compare to commonly used summaries in terms of CSR-model hypothesis discrimination power. We chose this test because CSR hypothesis is a stantard reference model of an early exploratory stage of pattern analysis.

4.1 Compared summaries

In addition to connectivity function C, cumulative connectivity function CC and clustering function c, we compute Ripley's K function, pair correlation function g, nearest neighbour distance distribution G, empty space function F, J function and triplet intensity T. See Table 1 for more details. We leave Q^2-statistics (Grabarnik and Chiu, 2002) off because they need parameter tuning, a task for which best practise is not yet established.

4.1.1 Estimation

We use the `R` software. The summaries K, g, G, F and J are estimated using package `spatstat` (Baddeley and Turner, 2005). The summaries C, CC, c and T are estimated using a package named `SGCS`, written by the author and which is available at `CRAN` (`http://cran.r-project.org`).

Calculation is carried out with $r \in [0, 0.3]$ discretised to $r_i = i \cdot 0.3/50$, $i = 0, ..., 50$. If not otherwise stated, border bias is corrected using reduced sample scheme. Simulation window is $[-0.3, 1.3]^2$ and the minimum distance from border $R_\ominus = 0.3$.

4.1.2 Power computation

We compare the summaries by their power to discriminate a non-CSR model from the CSR model. Write M_0 for CSR model, and M_1 for a challenger model. We estimate a *deviation test* (Illian et al., 2008, p. 457) based power

$$\gamma(\alpha) := \Pr(H_X > H_{0,\alpha} | X \sim M_1)$$

where $H_{0,\alpha}$ is chosen as the critical threshold value for fixed test size α, i.e. the value such that $\Pr(H_X > H_{0,\alpha} | X \sim M_0) = \alpha$. Then, after fixing α, we can compare the different statistics by their power.

We use as the statistic H the *deviations* under the M_0. For each summary function, say $F(r)$, estimate $F_0(r) \approx \bar{F}(r) = \frac{1}{N} \sum_{l=1}^{N} F_{X_l}(r)$ from simulated $X_1, ..., X_N \sim M_0$. Then we generate a realisation $Y \sim M_1$ from the competing model M_1, and estimate the model parameters, say $\hat{\theta}$, as if Y were from M_0 (just the λ in CSR model), and also estimate $F_Y(r)$. Then we compute the deviation

$$\Delta := \int_{r_{min}}^{r_{max}} |\bar{F}(r) - F_Y(r)|^\beta dr,$$

where $[r_{min}, r_{max}]$ is the range of parameter r and β is a priori fixed parameter defining the norm. We shall use $\beta = 2$ which gives the L^2-norm used in Cramér-von-Mises statistics. We also compute the deviation using $\beta = \infty$ i.e. maximum of absolute difference $\Delta' = \max |\bar{F}(r) - F_Y(r)|$.

After this we simulate $X_1, ..., X_K \sim M_0(\hat{\theta}_X)$ and compute $F_{X_i}(r)$ for each simulation, and using these values we compute the deviations under M_0

$$\Delta_i := \int_{r_{min}}^{r_{max}} |\bar{F}_0(r) - F_{X_i}(r)|^\beta dr, \quad i = 1, ..., K,$$

and also with the max-norm Δ_i'. Now, under M_0 the deviations $\Delta_i, \Delta_i', \Delta, \Delta'$ have discrete uniform distribution, so we can compute

$$\hat{p} := \Pr(\Delta > \Delta_{0,\alpha} | M_0) = \frac{1 + \sum_{i=1}^K \mathbf{1}(\Delta_i > \Delta)}{1 + K}.$$

We repeat the above procedure for several $Y_1, ..., Y_n \sim M_1$, and get $\hat{p}_1, ..., \hat{p}_n$. From these we estimate the power:

$$\gamma(\alpha) \approx \frac{\sum_{k=1}^n \mathbf{1}(\hat{p}_k < \alpha)}{n}$$

for each model and each summary.

4.2 Models for spatial point patterns

We use the following models to check the ends of regular-clustered axis (all models are assumed stationary and isotropic):

- Matern type II hardcore model, HC in short (Matérn, 1986)
- Poisson-Gaussian cluster model or Thomas model (Thomas, 1949)

And then the problematic mixture of clustered and regular behaviour,

- Cell model (Baddeley and Silverman, 1984).

Other models are

- Line segments-Cox process: stationary clustering in alignments (Illian et al., 2008, p. 383)
- Random intrusion model, RIM: We develop a process similar to the HC model but with additional 'intruders'.

Short description of each model and the chosen parameters follows, and are also summarised in Table 2.

4.2.1 Matérn type II hardcore model, HC in short

This is a thinned process: Start with Poisson realisation N_0 with intensity λ_0, mark the points independently $m(x_i) \sim U(0, 1)$, and then $N := \{x_i \in N_0 : \forall x_j \in N_0 \cap b(x_i, h) \text{ s.t. } m(x_j) < m(x_i)\}$.

The parameter h is chosen to be the maximum range on which the pattern can hold a wanted intensity. This is given by the thinned process intensity formula $\lambda = (1 - \exp(-\lambda_0 \pi h^2))/(\pi h^2)$. From this $\lambda_0 = -\log(1 - \lambda\pi h^2)/(\pi h^2)$, and the condition for maximum h comes from the requirement for the term inside log to be positive. For $\lambda = (50, 100, 200)$ this leads to the choises $h = (0.07, 0.05, 0.03)$.

4.2.2 Poisson-Gaussian cluster process i.e. Thomas-process

Start with Poisson process N_0 with intensity κ, and for each $x_i \in N_0$, create a normally distributed cluster of points $x_j \sim N(x_i, \sigma^2 I)$. We need two parameters: intensity of mother points κ and dispersion length σ. The number of daughters per cluster is then $\mu = \lambda/\kappa$. Next table shows the parameter configurations we used.

Type	Parameters
Few, large	$\kappa = 4, \sigma = c(0.08, 0.09, 0.10), \mu = \lambda/\kappa$
Many, small	$\kappa = 20, \sigma = c(0.03, 0.04, 0.05), \mu = \lambda/\kappa$

The model has 6 versions of which we use the $(\kappa = 20, \sigma = 0.04)$ and $(\kappa = 4, \sigma = 0.09)$ in comparisons to other models: The other versions were used to check that the two main classes don't vary much within. The first model with only few but large clusters will be referred to as Thomas1 and the second with many small clusters as Thomas2 in the results.

4.2.3 Cell process

This is a model with $n \times n$ cells, each cell having independently 0, 1 or 10 points with probability $1/10, 8/9, 1/90$, respectively, uniformly scattered within each cell. Mean number of points is 1 per cell, so we set the cell division per edge to be $\lfloor \sqrt{\lambda |W|} \rfloor$.

4.2.4 Line-segment Cox process

We generate a Poisson line segment process $S = \bigcup_l S_l$ with line length fixed to μ and mean line intensity λ_S. Then we sample Poisson$(\lambda_f \mu)$ points $\{x_{il}\}$ uniformly from each line, and the resulting $\mathbf{x} = \cup_l \cup_i x_{il}$ is the realisation, with mean intensity $\lambda = \lambda_S \cdot \lambda_f \cdot \mu$. We fix $\lambda_f = 10$ and try two situations, short segments $\mu = 0.1$ and long segments $\mu = 0.4$, referred to as Segments1 and Segments2, respectively.

4.2.5 Random intrusion model, RIM

Define a process such that 1) N_0 is a realisation of the HC process with intensity λ_0 2) For each $x_i \in N_0$, with probability p generate a neighbouring 'intruder' point distributed as $N(x_i, \sigma^2 I)$. This is similar to Poisson cluster models except the ground process is now a hard core model. The starting intensity is calculated as $\lambda_0 = \lambda/(1 + p)$. We use a version with $\sigma = 0.01$, i.e. intruders are close-by. The few intruders case, $p = 0.05$, is referred to as RIM1 and many intruders case, $p = 0.2$, as RIM2.

4.2.6 Estimated mean curves

Figure 2 depicts the mean curves for the graph theoretical summaries on the presented models, estimated from 10000 simulations. Cumulative connectivity function values are as expected for clustered Thomas1 and Segments1 above and for repulsive HC and RIM1 below CSR line. The Cell model values are at first identical to CSR values, but the relative regularity outside the small clusters forces the values below CSR curve after the cell size is reached at $r \approx 0.1$. Connectivity function values for Segments1 are below Thomas1 since two different segments can be almost parallel at a certain distance, contributing many path-disconnected pairs and lower values. The points in the small clusters of Cell model pair with non-path-connected points on the regular part, so the function value declines quick and the regularity induced nudge is well below those of HC and RIM1. The clustering function separates the clustered and repulsive models effectively, leaving the Cell model between. The short range behaviour of the curve is similar to that of clustered models, but after the small clusters are passed neighbour count increases more than triangle count and the curve levels below CSR curve, afterwhich it describes the major part of the model much like the regular models' curves.

4.3 Results

The emphasis of our analysis is on the graph based summaries. We simulate each model inside a window $[-0.3, 1.3]^2$ 1000 times, and compute the power of a test for the CSR hypothesis using size $\alpha = 0.05$. The range parameter r is sectioned into three distance classes, as some summaries are focused on short range features and are not good at longer ranges. The analysis is based on the values listed in Table 3 and depicted in Figure 3. Additionally, we comment on the pointwise envelopes which we omit from this paper (available online?). We report here the values when $\lambda = 100$ and the norm is the integral norm with $\beta = 2$. Differences to $\lambda = 50, 200$ and to the max-norm are reported in Appendix B. Finally, we will refer to Thomas1&2 as isotropically clustered, Segments1&2 as aligned clustered and the rest as non-clustered or regular.

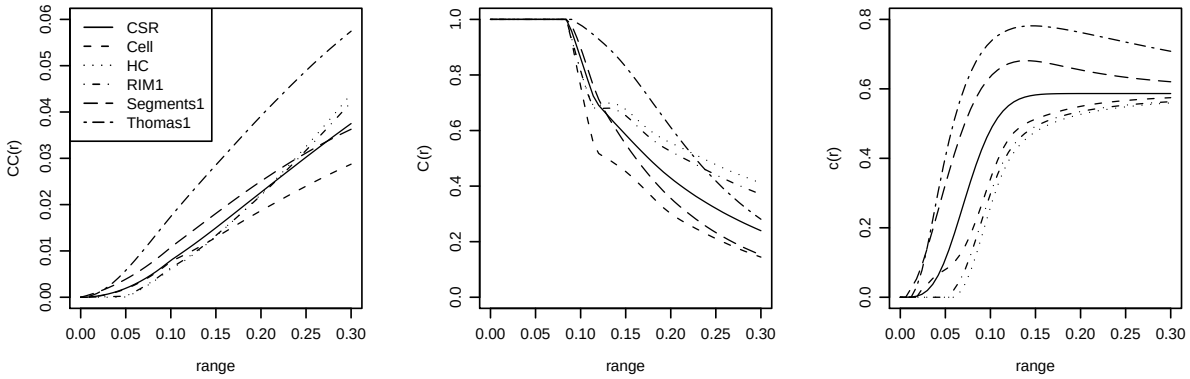

Figure 2: Estimated C, CC and c for models described in section 4, estimated from 10000 simulation.

4.3.1 Short range: $r \in [0 - 0.1]$

The power of C is low for all models with maximum 0.3 for Cell model. For the cluster models C has 0 power. This is likely because of the fixed $R = 1/\sqrt{\lambda} \approx 0.1$ range under which the function is constant (varies between realisations).

CC has better power, but in all cases less than K, even for the Cell model in which K has power ≈ 0.6. This is surprising as the theoretical K values in Cell and CSR are identical. Simulations show that CSR pointwise envelopes are contained in Cell model envelopes, so a likely reason for the power is detection of high variability exhibited by Cell model. Nevertheless CC is better than C but is generally poorer than others.

With the exception of the Cell model, K, g, G, F and J all have power > 0.9 so they are good in detecting deviation from CSR at short range. Clustering function c and triplet intensity T function are good with power > 0.9 for all except models RIM1&2 for which the T function stalls with powers 0.7 and 0.3 while c retains powers 0.9 and 0.8. The triangle count is possibly not low enough for T to work, whereas c factors in the hard core effect through small neighbour counts. For Cell model c has power 0.6 whilst T has power 1.0: The T envelopes contain CSR values completely so the model gives bigger variance to T, making the power good, whereas c has less variation and the power is poorer. Even though the c envelopes show the Cell structure, they are covered by the CSR envelopes.

4.3.2 Medium range: $r \in (0.1 - 0.2]$

C is a little better at this range, but power is > 0.5 only for isotropically clustered Thomas1&2 with 0.8 and 1.0. Third largest improvement is for the aligned cluster model Segments2, from 0.0 to 0.3. The clustered nature of these models is captured, but other summaries still do better. The envelopes imply that the variability for CSR is too large, probably due to the underlying component-giving graph.

CC is worse among all the models considered, power dropping from > 0.5 down to 0 for both HC and RIM1, and from > 0.7 down to 0.2 for RIM2 and Segments1. Segments2 stays above 0.6. K function also loses power, but only slightly, and is better than CC for all models with only two big drops: For Cell (from 0.6 to 0.3) and RIM1 (from 1.0 to 0.7). Why CC is poor has the same argument as for C: Envelopes get big due to the variability in the graph structure.

The c function stays good, being 0.7 for cell process and ≥ 0.9 for other models. This summary is overall best for non-clustered models, followed by K-function and further away T-function. In c the graph is calculated for each r so it differs from C and CC, resulting in a better picture of the graph-based topology of the pattern than just the one snapshot analysed by C and CC.

4.3.3 Long range: $r \in (0.2 - 0.3]$

C performs poorly again, only Thomas2 being 1.0, second best 0.3 for HC. CC is also worse than for medium range, only Thomas1&2 having power over 0.5. But c function triumphs: It beats the other summaries in all alternatives, being lowest 0.5 for Cell model, and second lowest at 0.8 for Segments2, when the second best summary for the same model is K with power only 0.3. It is actually odd that c works so well for the non-clustered models when the other summaries clearly don't. Maybe the interconnection of the graph at high ranges carries more information than previously assumed.

4.3.4 Conclusions for the whole range

Based on the limited selection of models in the study, C is not a good summary for finding evidence agains CSR hypothesis. The fixed graph structure must be bringing more uncertainty to the summary than is of benefit. The same applies to CC, especially at the medium range the variability increases and the envelopes fan out clearly more than in K function.

On the other hand c is very good, and for medium and long range it is best for all models, and for short range only RIM2 gives it some trouble (power still 0.8). The added information about the local intensity throught the neighbourhood size gives it more power when compared to the T function. Especially in the non-clustered models where the hardcore distances are present, c is much better than T.

The K function is also very good, in short and medium ranges it is in Top 3 and mostly in Top 2. At long ranges it is also one of the best, but the power drops for non-clustered models much below 0.5 (like all other summary except c). The pair correlation g is good at short ranges, but on longer ranges it's performance is mediocre, power being 0 for non-clustered models, excellent for Thomas2 and between 0.3-0.8 for less clustered models.

The F, G and J functions are good at short range, but useless for non-clustered at longer ranges, where the clearly isotropically clustered models are still easy for F whereas G and J stall.

5 Discussion

We studied three spatial point pattern summaries based on an imposed spatial graph structure. Two of these, cumulative connectivity function and clustering function, are new in point process context, and we analysed further the properties of the connectivity function introduced by Illian et al. (2008), p. 248.

The spatial graph based enrichment of point pattern analysis is similar to the methods based on random fields or tesselations, and is one of the approaches discussed by Illian et al. (2008). A graph classifies the points into components based on the edge relation. These components are then used as conditioning events in the summaries, resulting in second order descriptions inside the components. The added conditioning brings along theoretical problems, as the pathwise connectivity of two points is still one of the difficult open analytical questions in mathematical sciences. Also, the components come from a fixed parameter graph and are as such subject to depate. We discussed how to choose the parameter reasonably and in a way that comparisons of the values are possible. In addition, the clustering coefficient of conventional graph theory was converted to the spatial setting and modified to be a functional summary of the topology of a point pattern. It does not have a fixed component structure in which to measure two point correlations, but instead measures the relative connectivity strength of the points in neighbourhoods at different connection radii. Finally, a theoretical formula for the ratio unbiased version of clustering function for CSR model was presented, and the estimation of the summaries discussed.

After the introduction of the summaries we executed a simulation study where we compared the summaries power to discriminate various models from complete spatial randomness. We challenged the most common spatial summaries such as Ripley's K-function, nearest neighbour distribution and Baddeley's and van Lieshout's J-function on models including clustered and hardcore as well as some more complicated models.

The study showed that conditioning on a single geometric graph to emulate cluster structure results in high variation and does not lead to proper discrimination power. Connectivity function performs especially poorly on short ranges due to a inbuild blind area, and the improvement on longer ranges, which on some models is large, does not lead to a specifically good summary. Cumulative connectivity

function does a little better but also falls behind the renowned summaries. An marginal victory for both is of course on longer ranges and over the short range summaries, such as the nearest neighbour distance, where they have naturally little or no power at all.

But interestingly the clustering function, developed in graph theory, is the best summary in this study. It has a high power on all models, the difficult Cell model included, and is on long range and non-clustered models virtually supreme. The combination of second and third order moments seems to be an effective way to discriminate models, but similar to the J-function, this combining comes with the downside of interpretability. It is difficult to establish a spatial phenomenon to a certain value of the summary. To fully exploit the power of the summary the inter- or intra-connectivity of a point pattern on a certain 'scale' needs a proper spatial interpretation.

Further benefits of the approach is under study. The framework is suitable for more connection between graph theory and spatial statistics. For example, the definition of neighbourhood is simply a matter of changing the edge rule of the graph. A parameter free graph similar to Delauney triangulation could be used to find natural neighbourhoods e.g. in inhomogeneous forest plots or epidemiological case studies. Instead of the rigid geometric graph, adapted graphs for the clustering could help gain a more details of the pattern's nature.

6 Acknowledgements

The study is a part of doctoral studies and was funded by Jyväskylä Graduate School in Computing and Mathematical Sciences (COMAS), a grant from Finnish Academy of Science and Letters and Academy of Finland project No. 111156. The author would like to thank A. Penttinen and D. Stoyan for their comments, ideas and support.

References

Baddeley, A., Turner, R., 2005. Spatstat: an R package for analyzing spatial point patterns. Journal of Statistical Software 12 (6), 1–42, ISSN 1548-7660.
URL `www.jstatsoft.org`

Baddeley, A. J., Silverman, B. W., 1984. A cautionary example on the use of second-order methods for analysing point patterns. Biometrics 40, 1089–1093.

Chandler, S. A. G., 1989. Calculation of number of relay hops required in randomly located radio network. Electronic Letters 25, 1669–1671.

Daley, D. J., Vere-Jones, D., 2005. An Introduction to the Theory of Point Processes, 2nd Edition. Vol. 1. Springer.

Diggle, P., 1979. On parameter estimation and goodness-of-fit testing for spatial point patterns. Biometrics 35 (1).

Erdős, P., Rényi, A., 1959. On random graphs 1. Publ. Math. Debrecen (6), 290–297.

Grabarnik, P., Chiu, S. N., 2002. Goodness-of-fit test for complete spatial randomness against mixtures of regular and clustered spatial point processes. Biometrika (89), 411–421.

Illian, J., Penttinen, A., Stoyan, H., Stoyan, D., 2008. Statistical analysis and modelling of spatial point patterns. Wiley.

Marchette, D. J., 2004. Random graphs for statistical pattern recognition. Wiley.

Matérn, B., 1986. Spatial variation, 2nd Edition. Lecture notes in statistics. Springer-Verlag.

Mecke, K. R., Stoyan, D., 2005. Morphological characterization of point patterns. Biometrical Journal 47 (4), 473–488.

Møller, J., Waagepetersen, R. P., 2003. Statistical inference and simulation for spatial point processes. Chapman & Hall/CRC.

Okabe, A., Boots, B., Sugihara, K., Chiu, S. N., 2000. Spatial Tessellations: Concepts and Applications of Voronoi Diagrams, 2nd Edition. Wiley.

Penrose, M., 2003. Random geometric graphs. Oxford university press.

Ripley, B. D., 1976. The second-order analysis of stationary point processes. J. Appl. Probab. 13, 255–266.

Ripley, B. D., 1977. Modelling spatial patterns. JRSS Series B 39, 172–212.

Schladitz, K., Baddeley, A. J., 2000. A third order point process characteristic. Scand. J. Stat. 27, 657–671.

Stoyan, D., Kendall, W. S., Mecke, J., 1995. Stochastic geometry and its applications, 2nd ed. Wiley.

Stoyan, D., Stoyan, H., 1994. Fractals, random shapes and point fields: methods of geometrical statistics. John Wiley and Sons.

Ta, X., Mao, G., Anderson, B. D. O., 2007. On the probability of k-hop connection in wireless sensor networks. IEEE Communication letters 11 (9), 662–664.

Thomas, M., 1949. A generalization of poisson's binomial limit for use in ecology. Biometrika 36, 18–25.

van Lieshout, M. N. M., Baddeley, A. J., 1996. A nonparametric measure of spatial interaction in point patterns. Statistica Neerlandica 50, 344–361.

Watts, D., Strogatz, S., 1998. Collective dynamics of 'small-world' networks. Nature 393, 440–442.

A Tables and Figures

Table 1: Summaries computed in the simulation study.

Functional	Symbol	Description
Ripley's [1]	K	Number of r-pairs with o as vertex.
Pair correlation[2]	g	Prob. a point at range r from o is $\lambda g(r) dod\mathbf{r}$
Nearest neigh. dist.[3]	G	Dist. of range from $o \in N$ to nearest neighbour.
Empty space[4]	F	Dist. of range from $o \in W$ to nearest point in N.
J-function[5]	J	Ratio of G and F.
Triplet intensity[6]	T	N. of triangles with $o \in N$ as vertex.
Connectivity[7]	C	Prob. of r-pair points are in same component.
Cumul. connectivity	CC	N. of r-pairs that are also path-connected.
Clustering function	c	Portion of 2-connected neighbours of o.

References: 1. Ripley (1976), 2.Stoyan and Stoyan (1994), 3.Diggle (1979), 4. Ripley (1977) 5. van Lieshout and Baddeley (1996), 6. Schladitz and Baddeley (2000), 7. Illian et al. (2008).

Table 2: Models and free variables after intensity fixes others.

Model	Shorthand	Parameters
Poisson	CSR	-
Matern type II hard-core	HC	-
Poisson-Gaussian cluster: Few Big	Thomas1	$\kappa = 4, \sigma = 0.09$
Poisson-Gaussian cluster: Many Small	Thomas2	$\kappa = 20, \sigma = 0.04$
Regular-cluster Cell model	Cell	-
Segment-Cox: Short segments	Segments1	fiber length $\mu = 0.1$
Segment-Cox: Long segments	Segments2	fiber length $\mu = 0.4$
Random intrusion: few intruders	RIM1	$p = 0.05$, $\sigma = 0.05$
Random intrusion: many intruders	RIM2	$p = 0.2$, $\sigma = 0.05$

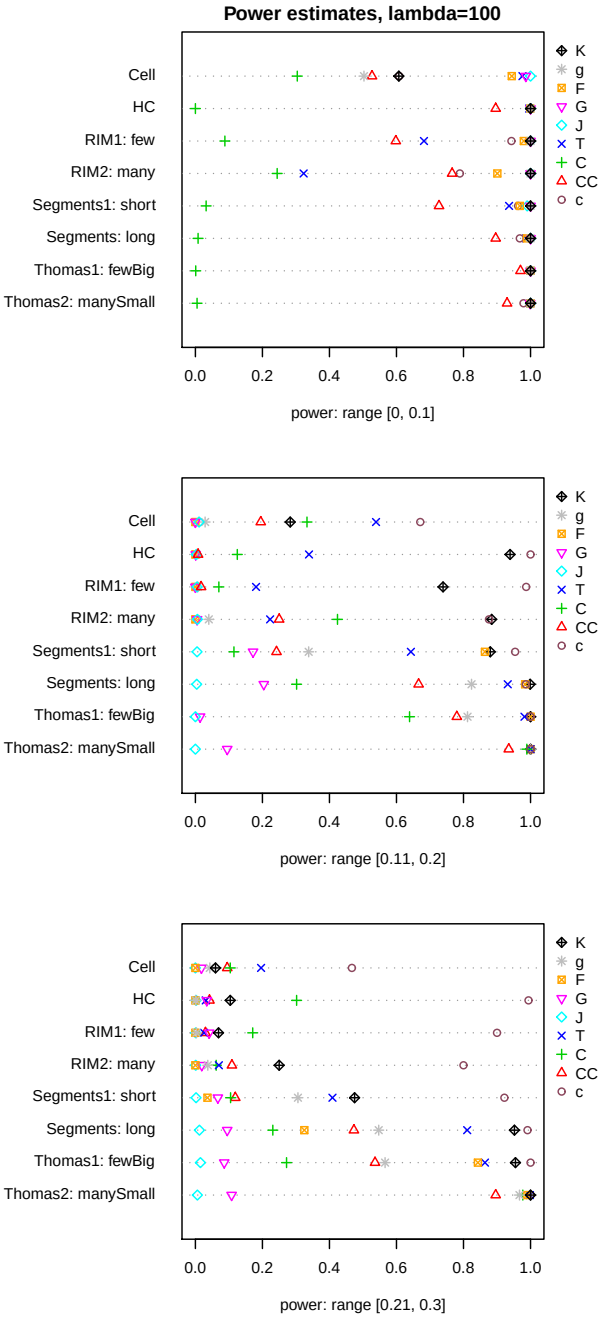

Figure 3: Separation power estimated from significant deviation-tests against the CSR-values. Individual test size $\alpha = 0.05$, intensity of patterns $\lambda = 100$, integral-norm. Three r-ranges, $[0, 0.1], [0.11, 0.2]$ and $[0.21, 0.3]$ are presented separately from top to bottom. In each plot, horizontal lines correspond to considered models, and symbols on each line correspond to different summaries. The more on the right the symbol is, the higher is the corresponding summary's estimated power.

B Other results

B.1 Differences with $\lambda = 200$ trial

To counter the effect of change in the ranges which affects especially nearest neighbour and empty space estimation, we scale the ranges by putting $\lambda K(r)$ fixed for CSR, so the ranges become scaled with $\sqrt{100/200}$ leading roughly to test $[0, 0.07]$ for small, $[0.07, 0.14]$ for medium and $[0.14, 0.21]$ for large

Table 3: Separation power estimated from significant deviation-tests against the CSR-values. Individual test size $\alpha = 0.05$, intensity of patterns $\lambda = 100$, integral-norm. Three r-ranges, $[0, 0.1]/[0.11, 0.2]/[0.21, 0.3]$.

	K	g	F	G	J
Cell	0.6/0.3/0.1	0.5/0.0/0.0	0.9/0.0/0.0	1.0/0.0/0.0	1.0/0.0/0.0
HC	1.0/0.9/0.1	1.0/0.0/0.0	1.0/0.0/0.0	1.0/0.0/0.0	1.0/0.0/0.0
RIM1	1.0/0.7/0.1	1.0/0.0/0.0	1.0/0.0/0.0	1.0/0.0/0.0	1.0/0.0/0.0
RIM2	1.0/0.9/0.2	1.0/0.0/0.0	0.9/0.0/0.0	1.0/0.0/0.0	1.0/0.0/0.0
Segments1	1.0/0.9/0.5	1.0/0.3/0.3	1.0/0.9/0.0	1.0/0.2/0.1	1.0/0.0/0.0
Segments2	1.0/1.0/1.0	1.0/0.8/0.5	1.0/1.0/0.3	1.0/0.2/0.1	1.0/0.0/0.0
Thomas1	1.0/1.0/1.0	1.0/0.8/0.6	1.0/1.0/0.8	1.0/0.0/0.1	1.0/0.0/0.0
Thomas2	1.0/1.0/1.0	1.0/1.0/1.0	1.0/1.0/1.0	1.0/0.1/0.1	1.0/0.0/0.0

	T	C	CC	c
Cell	1.0/0.5/0.2	0.3/0.3/0.1	0.5/0.2/0.1	0.6/0.7/0.5
HC	1.0/0.3/0.0	0.0/0.1/0.3	0.9/0.0/0.0	1.0/1.0/1.0
RIM1	0.7/0.2/0.0	0.1/0.1/0.2	0.6/0.0/0.0	0.9/1.0/0.9
RIM2	0.3/0.2/0.1	0.2/0.4/0.1	0.8/0.2/0.1	0.8/0.9/0.8
Segments1	0.9/0.6/0.4	0.0/0.1/0.1	0.7/0.2/0.1	1.0/1.0/0.9
Segments2	1.0/0.9/0.8	0.0/0.3/0.2	0.9/0.7/0.5	1.0/1.0/1.0
Thomas1	1.0/1.0/0.9	0.0/0.6/0.3	1.0/0.8/0.5	1.0/1.0/1.0
Thomas2	1.0/1.0/1.0	0.0/1.0/1.0	0.9/0.9/0.9	1.0/1.0/1.0

ranges. Note that even though the parameters of HC (min. distance) and Cell (min. dist + cluster radius) scale with λ the dispersion σ of Thomas1&2 and RIM1&2 does not. So in the latter models the clusters are relatively larger for the higher intensity models even after scaling.

Short range: We see improvement in power of C for clustered models, Thomas1&2 rises from 0 to 0.7 and Segments2 from 0 to 0.3. For Cell model the power is not increased but C drops 0.2 digits. Other models show better power for all summaries. In conclusion C benefits greatly from the increased accuracy, others improve a bit.

Medium range: C gains 0.4 points of power for Thomas1, and there are some minor improvements of size 0.1-0.2 for CC and c. G function gains 0.1-0.3 power, but F almost 1.0 for regular models: The regularity stabilises F to 1 for ranges above ≈ 0.1, and in our CSR simulation the maximum envelope reaches 1 only after range $\approx$0.14, as the CSR model allows for small amount of highly isolated points. Of others, T function power jumps from 0.2 to 0.9 for RIM1, and others gain a little more power.

Long ranges: C gains again power for Thomas1, from 0.3 to 0.8, not much change in other models. CC gains 0.1–0.2 power on all models, no big jumps. c is still best with slightly improved (+0.2) power for Cell model, staying above of even K function which gains 0.7 for RIM1 and ≈ 0.1 for others.

B.2 Differences with $\lambda = 50$ trial

The ranges used here where [0.0.14] and $[0.0.14, 0.28]$. We skip the long distance as it goes above our original r_{max}.

Short range: C drops below 0.1 for all models. CC loses power too, especially with HC and RIM2 power drop from 0.9 and 0.8 to 0.3 and 0.2. c stalls for RIM2, 0.8 to 0.2, but behaves well on others not like it's best rival T, which drops from 1.0, 0.7 and 0.3 well below 0.1 for HC, RIM1 and RIM2 respectively, and from 1.0 to 0.5 for Cell. F also stalls with Cell model, drop from 0.9 to 0.1, and with RIM2, from 0.9 to 0.2. Also, J loses power for Segments2, drop from 1.0 to 0.3. K, G and g change less than 0.1 if any.

Medium range: C loses power on all models except HC (stays at 0.1). CC also loses power, drops are 0.1-0.3 points. All summaries crash on RIM2, but c still stays atop with 0.3 power. The c also stays unchanged for HC when K and T drop from 0.9 and 0.4 to 0.4 and 0.1. Overall, slight loss of power is visible on all summaries on all models, least on c.

B.3 Differences between norms

Here's a short rundown of the differences between the norms.

Short range: The C-function has more power with the max-norm, especially the clustered segments and Thomas process power rises from $\sim$0 upto 0.5 (Thomas2). The J-function for both Segments1&2 drop from $\approx$1 to 0.15 and 0.6 with max-norm. The CC also has less power with max-norm, only Thomas1&2 don't suffer. The c-function improves from $\sim$0.8 to $\sim$0.9 for RIM2. Other values do not change more than 0.05.

Medium range: K-function has lower power with max-norm for HC, RIM1&2, change $\sim$ -0.3. C-function improves for RIM1 from $\sim$0.4 to $\sim$0.6, but c declines from 0.9 to 0.7. c is also on all other models $\sim$ -0.05 worse with max-norm. Other summaries stay pretty much the same.

Long range: No noticable changes.

Conclusion: The change of norm has an influence on the new summaries at short ranges. The influence is small but favourable for C and c, and negative for CC. C benefits most on the cluster models. The biggest drops in power of CC are for non-clustered processes (Cell, HC, RIM).